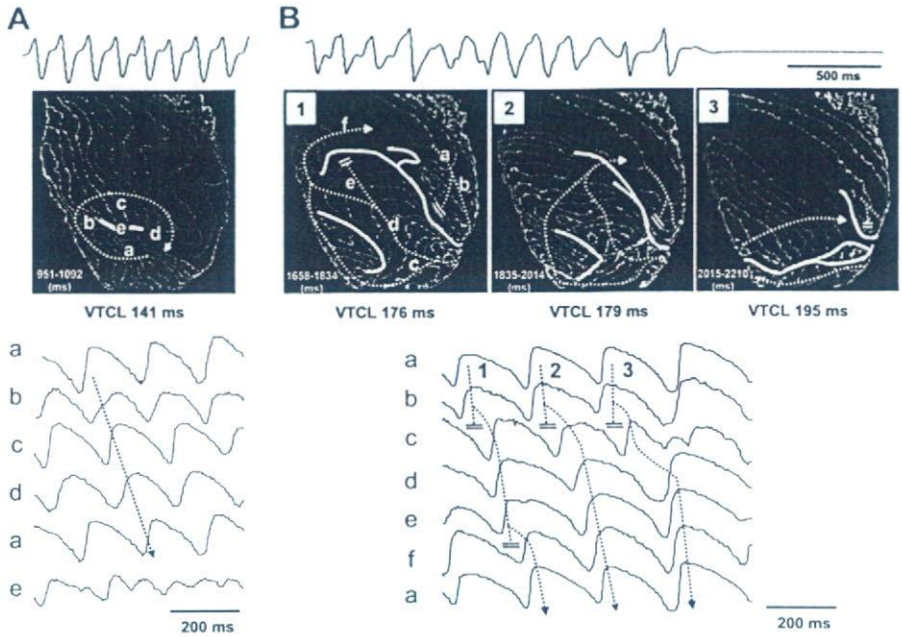

図5　ニフェカラント(NF 0.1 μM)添加前後のスパイラル興奮

A：コントロールで誘発したVT(ほぼ単形性)中の興奮伝播(上段は双極心電図，中段は左室前面の興奮伝播等時線図，下段は旋回経路の活動電位シグナル)．等時線は5.33 ms間隔で表示した(緑色は先行する興奮前面，青色は後続する興奮前面を表す)．興奮は左室前面ほぼ中央の線状の機能的ブロックライン(FBL，黄色)の周囲を時計方向に旋回している．活動電位の光学シグナルは，等時線図上に示す5点(a～e)から得られた波形を示す．

B：ニフェカラント添加後に誘発した多形性VT中の興奮伝播(上段は双極心電図，中段は連続する3拍の興奮伝播等時線図，下段は旋回経路の活動電位シグナル)．興奮は，2本の長い複雑な形状の機能的ブロックライン(黄色)の周りをほぼ時計方向に旋回しているが，その経路は一拍ごとに変化している．活動電位の光学シグナルは，等時線図上に示す6点(a～f)から得られた波形を示す．　〔文献5)より引用改変〕

フェカラント作用下で誘発した19 VTについて，スパイラル興奮が自然停止するメカニズムを解析した[5]．コントロールでは，逆方向に旋回する二つのスパイラル興奮が相互に衝突することで停止する場合(mutual annihilation)が大部分(9/10，90%)であり(図7A)，残りの1例では単一スパイラルが房室間溝に衝突して停止した．ニフェカラント作用下では，過半数(12/19，63%)でスパイラル興奮が大きなmeanderingを示した後，房室間溝に衝突して停止した(図7B)．残りの6例では，スパイラル興奮の旋回中心が，それ自身の不応期領域に囲まれて興奮間隙が消失することにより停止した[5]．前者には，ニフェカラントによる旋回運動のunpinningが重要な役割を果たしており，後者は旋回中心付近の活動電位再分極の遅延に起因すると考えられる．

Ⅳ．内向き整流K^+チャネルの役割

心室スパイラル・リエントリーの旋回中心付近の活動電位再分極に，どのイオンチャネル電流が主要な役割を果たすかについては，研究者によって意見が分かれている．ニフェカラントを用いたわれわれの実験結果からは，心室スパイラル興奮では遅延整流型K^+電流(I_K)の速い活性化成分(I_{Kr})が旋回中心から離れた部分(arm)だけでなく，旋回中心付近の興

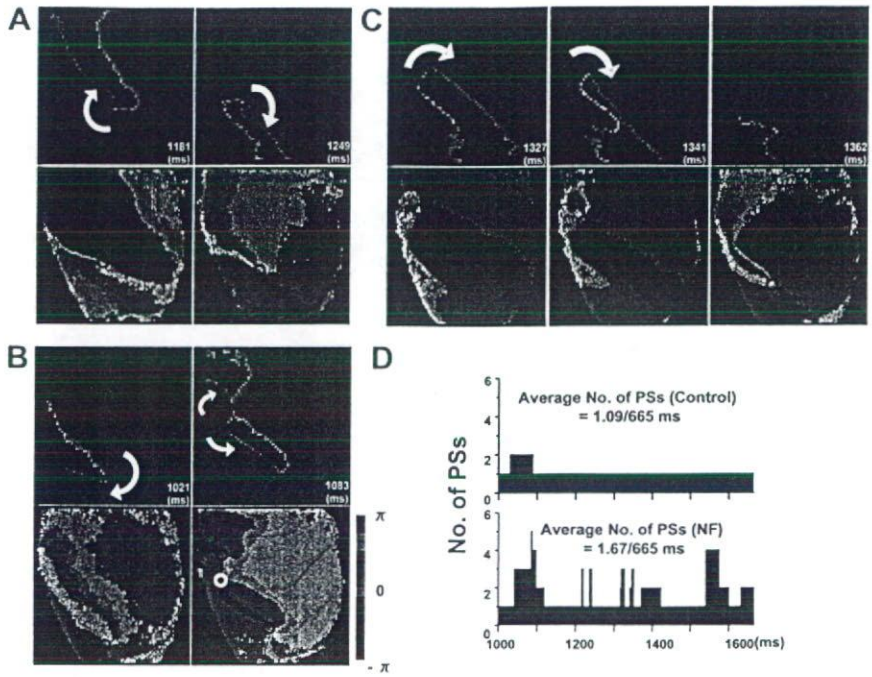

図6　興奮前面(wave front)と後面(再分極終末wave tail)の相互作用による興奮波面の分裂(wavebreak formation)

A：コントロールで誘発したVT中のwave front(赤)とwave tail(緑)の動き(上段)と，それに対応する位相マップ(下段)．Wave frontがwave tailを追いかけているが，それらが遭遇することはない(wavebreakは発生しない)．

B：ニフェカラント(0.1 μM)添加後に誘発したVT中のfront-tail相互作用で発生したスパイラル興奮の分裂(breakup)．Wave frontがwave tailに衝突して，新たに二つの旋回中心が発生している．

C：ニフェカラント後のVT中のfront-tail相互作用で生じた旋回中心の突然の移動．位相マップ上の丸印は旋回中心を示す(黒丸は時計回転，白丸は反時計回転)．

D：観察領域(左心室前面)における位相特異点(PS)の数(/665 ms)の推移(上段はコントロール，下段はニフェカラント添加後のVT)．　〔文献5)より引用改変〕

奮の再分極にも深くかかわっており，それらのダイナミクスを制御し，停止させるための標的電流となることが示唆される[5)~7)]．Quら[25),26)]は，Luo-Rudy心筋細胞モデル(phase 1)を用いた二次元興奮媒体のコンピュータシミュレーションで，スパイラル中心でもI_Kは十分に保たれており，I_Kコンダクタンスの低下がスパイラル興奮の著しいmeanderingとbreakup，あるいは早期停止をもたらすことを報告している．一方，BeaumontとJalife[27)]は，独自の心筋細胞モデルを用いたシミュレーションで，スパイラルの旋回中心ではAPDが著しく短縮しており，活動電位の再分極に対するI_Kの関与は少ないことを示し，スパイラル興奮を制御するための標的電流としてはI_Kよりも内向き整流Kチャネル電流(I_{K1})が重要であると主張している．

図8は，Samie, Jalifeら[18)]がmother rotorタイプのVF成立機転におけるI_{K1}の重要性を提唱した実験結果の一部である．モルモットの心臓にバースト刺激を加えて持続性のVFを誘発し，光学マッピングで膜電位シグナルの周波数成分解析を行うと，最も速い主要周波数(dominant frequency：DF)領域は，常に左室前面に現れた．そして，しばしばこの領域

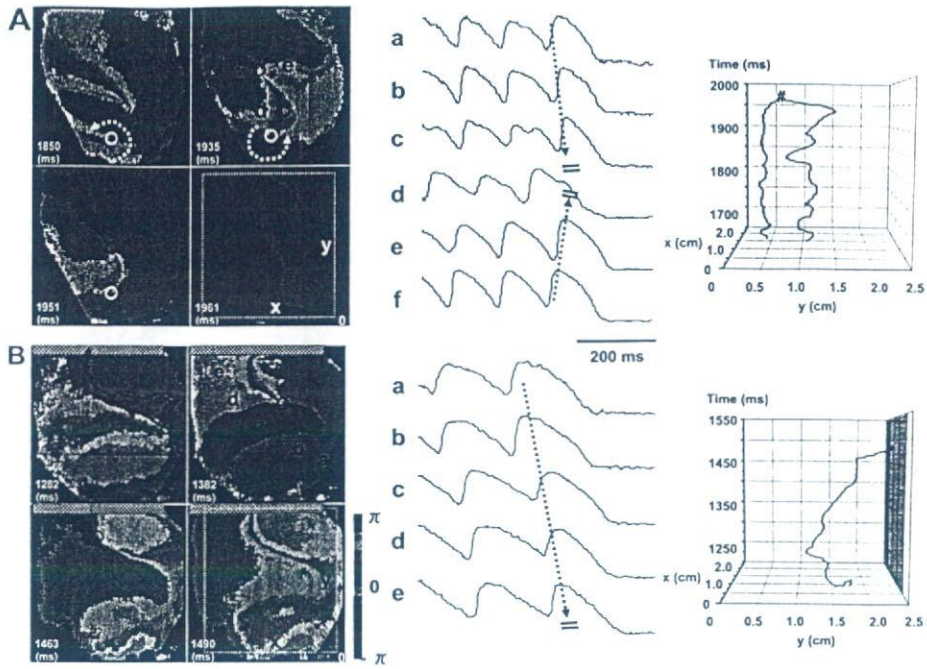

図7　スパイラル・リエントリーの停止様式

A：コントロールのVT自然停止；逆方向に回転する一組のスパイラル興奮が相互に衝突して停止している(mutual annihilation)．左はVT最終拍の位相マップ(4コマ表示)；丸印は旋回中心を示す(黒丸は時計回転，白丸は反時計回転)．中央は位相マップ上の6ヵ所(a～f)の活動電位シグナル．右は二つの位相特異点(PS)の空間(x, y)—時間(time)軌跡；赤は時計回転，青は反時計回転を表す．

B：ニフェカラント作用下のVT自然停止；スパイラル興奮が房室間溝に衝突して停止している．左はVT最終拍の位相マップ(4コマ表示)；各フレームの上端は房室間溝を示す．赤い矢印は旋回中心(PS)移動の軌跡を示す．中央は位相マップ上の5ヵ所(a～e)の活動電位シグナル．右は位相特異点(PS)の空間(x, y)—時間(time)軌跡；青い壁は房室間溝を表す．〔文献5)より引用改変〕

に一致して高速で旋回するスパイラル・リエントリー(mother rotor)が出現し，そこから周囲に向かって広がる興奮伝播が複雑にブロックされる様子(fibrillatory conduction)が観察された．彼らは，この研究で単離心筋細胞の膜電位固定実験と，二次元心筋組織を想定したコンピュータシミュレーションを行い，左室が右室に比べてI_{K1}の外向き成分が大きいため，スパイラル旋回中心付近の活動電位再分極が促進され，きわめて高速で安定した旋回興奮運動が可能になると結論している．

Warren, Jalifeら[28]は，同様なモルモット心臓のVF誘発実験で，I_{K1}遮断作用をもつBa^{2+}の効果を検討している(図9)．その結果，心室筋細胞の外向きI_{K1}電流を減らし，APDを延長させる濃度のBa^{2+}(10～50 μM)がVF時の左室前面に存在する最大DF領域の周波数を著しく低下させるとともに，VFの停止を促すことが判明した．しかし，Ba^{2+}には，VFを停止させるが，VFに代わる遅い興奮頻度の多形性VTをもたらす作用があることも示された[27]．

最近Noujaim, Jalifeら[29]は，心臓特異的にKir2.1(I_{K1}チャネルの主要構成蛋白)を過剰発現するトランスジェニックマウス(TG)を用いた実験で，摘出心臓の膜電位光学マッピングを行い，I_{K1}がVT/VF成立に果たす役割を検討している．その結果，①TG

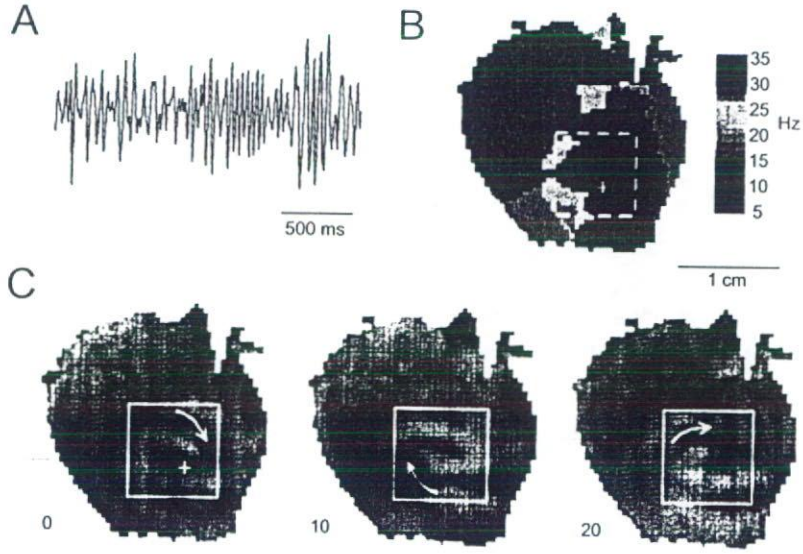

図8　モルモット心室に誘発したVF中に観察された高速旋回興奮

A：VF中の心電図波形.

B：VF中の主要周波数(dominant frequency, DF)マップ；左室と右室でDF分布に勾配がある(左室のDFが高い).

C：左室前面に中心をもつ時計方向の旋回興奮(数値はms).

〔文献18)より引用改変〕

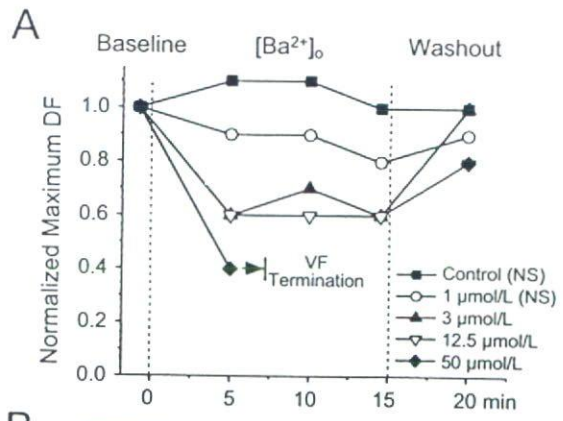

B

$[Ba^{2+}]_o$	VF Termination
1 μmol/L	0 %
3 μmol/L	20 %
12.5 μmol/L	33 %
50 μmol/L	100 %

図9　モルモット心室に誘発したVFに対するBa^{2+}の作用

A：主要周波数(DF)マップ上の最大周波数の変化(baselineで正規化)；Ba^{2+}添加により，濃度依存性に最大周波数が減少し，Ba^{2+}を除去すると元に戻っている.

B：Ba^{2+}添加後のVF停止率.　〔文献28)より引用改変〕

マウスでは野生型(WT)マウスに比べて，誘発されたVT/VFの持続時間が著しく長く，周期が短いこと，②VT/VF中の心室DFマップでは，TGマウスのほうがWTマウスよりも，はるかに高い周波数領域をもつこと，③TGマウスが有するこれらの特徴が，I_{K1}遮断作用をもつBa^{2+}添加により消失することが示された.

V．心室細動治療におけるK^+チャネル遮断の役割

スパイラル・リエントリーがVFの成立にどのようにかかわるかについては，現在二つの考え方がある(mother rotor仮説とdynamic wavebreak仮説)[15)~19)]. Mother rotor仮説では，心室の一部(不応期の短い部分)に限られた数の速い回転を示す旋回興奮(rotor)があり，そこがエンジンとなって，周期の短い興奮が発生し，周辺に不規則に伝播する(fibrillatory conduction)ことが本体であると考えられている[17)~19)]. 一方，dynamic wavebreak仮説(あるいはcontinuous wavebreak仮説)では，興奮波の分裂に

よって端の切れた波面が自己増殖的に繰り返し発生することが細動の本体であり，エンジンに相当するmother rotorの存在は必ずしも必要はないとされている[15,16]．最近では，これら二つの概念は相反するものではなく，相補的であり，病態や心筋組織の状態によって両者の寄与が異なるとする考え方が主流となってきた[30]．Chenら[30]は，臨床で観察されるVFには興奮頻度の速いタイプIと興奮頻度の遅いタイプIIがあり，前者が急峻なAPD回復曲線によるdynamic wavebreakを基盤としており，後者は興奮性低下と組織の不均一性増大を基盤とする(mother rotorとfibrillatory conductionの成立を促す)可能性が大きいと述べている．VFは最初はタイプIとして発生することが多いものの，それが持続すると心筋虚血が進行し，タイプIIへと移行する．冠動脈疾患をはじめとする器質的心臓病やNa^+チャネル遮断薬の存在は，タイプIIへの移行を促し，DCショックによる除細動を困難にする[30]．

Mother rotorタイプのVFが持続するためには，エンジンとなるスパイラル・リエントリーの中心が心室の一部(解剖学的な不連続性)にpinningもしくはanchoring必要がある[31]．ニフェカラントをはじめとする，I_{Kr}チャネル遮断薬は，スパイラル・リエントリーのpinningを妨げ，それを速やかに移動させることで早期停止を促し，VFに対するある程度の治療効果，防止効果が期待できる．しかし，一方では興奮前面がそれ自身の終末部と相互作用する機会が増し(front-tail interaction)，興奮波面の分裂を促すことで，VTからVFに移行しやすくなる(dynamic wavebreakを基盤とする細動を悪化させる)危険性をもたらす．I_{K1}遮断作用をもつBa^{2+}に同様な作用があるかどうかは，まだ検証されていない．

VFに対する最も有効な治療法は，現時点ではDCショックである．DCショックは心室全体に強い電流を与え，既存の興奮をいったんすべて止めて，その興奮位相をそろえる(phase reset)ことで，正常の調律を回復させる手段である[32]．しかし，DCショックには，仮想電極効果(virtual electrode polarization)

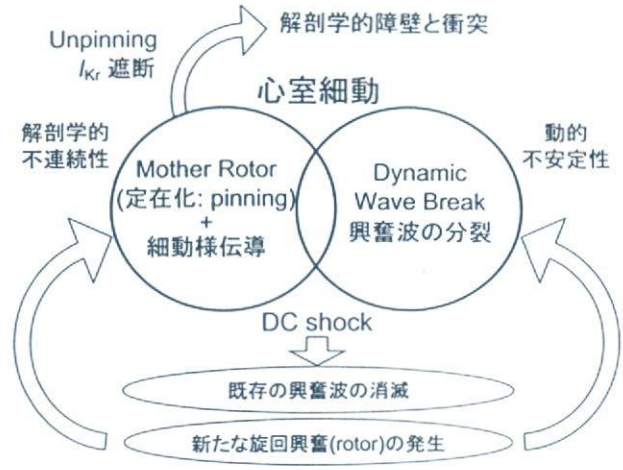

図10　二種類のVF維持機構とDCショックおよびニフェカラントの効果

によって，新たにスパイラル興奮を作り出す作用があり[33]，このスパイラルが分裂・生成を繰り返すようになったり(dynamic wavebreak)，ある特定の部位にpinningしてmother rotorを形成すると，新しいVFが発生する(除細動不成功)[31]．I_{Kr}チャネル遮断薬は，スパイラル・リエントリーのpinningを防ぐことで(unpinning：抜錨)mother rotorタイプのVFの成立をふせぎ，DCショックの成功率を高めると考えられる(図10)．I_{K1}チャネル遮断薬作用をもつBa^{2+}にもDCショックの成功率を高める作用があることが報告されている[34]．これらのK^+チャネル遮断操作は，おそらく共通のメカニズム(unpinning)によりDCショックの除細動効果を高め，electrical storm[35]からの脱却を促す効果を発揮すると推測される．

〔文　　献〕

1) Jalife J : Ventricular fibrillation. Mechanisms of initiation and maintenance. Annu Rev Physiol, 2000 ; 62 : 25～50
2) Samie FH, Jalife J : Mechanisms underlying ventricular tachycardia and its transition to ventricular fibrillation in the structurally normal heart. Cardiovasc Res, 2001 ; 50 : 242～250
3) Weiss JN, Garfinkel A, Karagueuzian HS, Qu Z, Chen P-S : Chaos and the transition to ventricular fibrillation. A

new approach to antiarrhythmic drug evaluation. Circulation. 1999 ; 99 : 2819～2826
4) Weiss JN, Qu Z, Chen P-S, Lin S-F, Karagueuzian HS, Hayashi H, Garfinkel A, Karma A : The dynamics of cardiac fibrillation. Circulation. 2005 ; 112 : 1232～1240
5) Yamazaki M, Honjo H, Nakagawa H, Ishiguro YS, Okuno Y, Amino M, Sakuma I, Kamiya K, Kodama I : Mechanisms of destabilization and early termination of spiral wave reentry in the ventricle by a class Ⅲ antiarrhythmic agent, nifekalant. Am J Physiol Heart Circ Physiol. 2007 ; 292 : H539～H548
6) Amino M, Yamazaki M, Nakagawa H, Honjo H, Okuno Y, Yoshioka K, Tanabe T, Yasui K, Lee J-K, Horiba M, Kamiya K, Kodama I : Combined effects of nifekalant and lidocaine on the spiral-type re-entry in a perfused 2-dimensional layer of rabbit ventricular myocardium. Circ J. 2005 ; 65 : 576～584
7) Honjo H, Yamazaki M, Kamiya K, Kodama I : Modulation of spiral wave reentry by K⁺channel blockade (review). Circ J. 2007 ; 71 (Suppl A) : A26～A31
8) Murakawa Y, Yamashita T, Kanese Y, Omata M : Can a class Ⅲ antiarrhythmic drug improve electrical defibrillation efficacy during ventricular fibrillation? J Am Coll Cardiol. 1997 ; 29 : 688～692
9) Miyoshi M, Yasuda S, Miyazaki S, Ueno K, Morii I, Satomi K, Otsuka Y, Kawamura A, Kurita T, Kitamura S, Monogi H : Intravenous administration of nifekalant hydrochloride for the prevention of ischemia-induced ventricular tachyarrhythmia in patients with renal failure undergoing hemodyalysis. Circ J. 2003 ; 67 : 898～900
10) Nakaya H, Tohse N, Takeda Y, Kanno M : Effects of MS-551, a new class Ⅲ antiarrhythmic drug, on action potential and membrane currents in rabbit ventricular myocytes. Br J Pharmacol. 1993 ; 109 : 157～163
11) Nakaya H, Uemura H : Electropharmacology of nifekalant, a new class Ⅲ antiarrhythmic drug. Cardiovasc Drug Re. 1998 ; 16 : 133～144
12) Yoshioka K, Amino M, Morita S, Nakagawa Y, Usui K, Sugimoto A, Matsuzaki A, Deguchi Y, Yamamoto I, Inokuchi S, Ikari Y, Kodama I, Tanabe T : Can nifekalant hydrochloride be used as a first-line drug for cardiopulmonary arrest (CPA)? : Comparative study of out-of-hospital CPA with acidosis and in-hospital CPA without acidosis. Circ J. 2006 ; 70 : 21～27
13) Roden DM : Drug-induced prolongation of the QT interval. N Engl J Med. 2004 ; 350 : 1013～1022
14) Pertsov AM, Davidenko JM, Salomonsz R, Baxter WT, Jalife J : Spiral waves of excitation underlie reentrant activity in isolated cardiac muscle. Circ Res. 1993 ; 72 : 631～650
15) Garfinkel A, Chen P-S, Weiss JN, et al : Nonlinear dynamics of excitation and propagation in cardiac muscle. In : Zipes DP, Jalife J, eds. Cardiac Electrophysiology : From Cell to Bedside. 3rd ed. WB Saunders, Philadelphia, 2000 ; 315～320
16) Qu Z, Garfinkel A : Nonlinear dynamics of excitation and propagation in cardiac muscle. In : Zipes DP, Jalife J, eds. Cardiac Electrophysiology : From Cell to Bedside. 4th ed. WB Saunders, Philadelphia, 2004 ; 327～335
17) Chen J, Mandapati R, Berenfeld O, Skanes AC, Jalife J : High-frequency periodic sources underlie ventricular fibrillation in the isolated rabbit heart. Circ Res. 2000 ; 86 : 86～93
18) Samie FH, Berenfeld O, Anumonwa J, Mironov SF, Udassi S, Beaumont J, Taffet S, Pertsov AM, Jalife J : Rectification of the background potassium current. A determinant of rotor dynamics in ventricular fibrillation. Circ Res. 2001 ; 89 : 1216～1223
19) Jalife J : Dynamics and molecular mechanisms of ventricular fibrillation in normal hearts. In : Zipes DP, Jalife J, eds. Cardiac Electrophysiology : From Cell to Bedside. 4th ed. WB Saunders, Philadelphia, 2004 ; 390～398
20) Pertsov AM, Jalife J : Three-dimensional vortex-like reentry. In : Zipes DP, Jalife J, eds. Cardiac Electrophysiology : From Cell to Bedside. 2nd ed. WB Saunders, Philadelphia, 1995 ; 403～410
21) Efimov IR, Sidorov V, Cheng Y, Wollenzier B : Evidence of three-dimensional scroll waves with ribbon-shaped filaments as a mechanism of ventricular tachycardia in the isolated rabbit heart. J Cardiovasc Electrophysiol. 1999 ; 10 : 1452～1462
22) Pertsov AM, Jalife J : Scroll waves in three-dimensional cardiac muscle. In : Zipes DP, Jalife J, eds. Cardiac Electrophysiology : From Cell to Bedside. 3rd ed.WB Saunders, Philadelphia, 2000 ; 336～344
23) Weiss JN, Chen PS, Qu Z, Karagueuzian HS, Garfinkel A : Ventricular fibrillation : how do we stop the waves from breaking? Circ Res. 2000 ; 87 : 1103～1107
24) Weiss JN, Qu Z, Chen PS, Lin SF, Karagueuzian HS, Hayashi H, Garfinkel A, Karma A : The dynamics of cardiac fibrillation. Circulation. 2005 ; 112 : 1232～1240
25) Qu Z, Xie F, Garfinkel A, Weiss JN : Origins of spiral wave meander and breakup in a two-dimensional cardiac tissue model. Ann Biomed Eng. 2000 ; 28 : 755～771
26) Qu Z, Weiss JN : Effects of Na⁺and K⁺channel blockade on vulnerability to and termination of fibrillation in simulated normal cardiac tissue. Am J

Physiol Heart Circ Physiol. 2005 ; 289 : H1692～H1701
27) Beaumont J, Jalife J : Rotors and spiral waves in two dimensions. In : Zipes DP, Jalife J, eds. Cardiac Electrophysiology : From Cell to Bedside. 3rd ed. WB Saunders, Philadelphia, 2000 ; 327～335
28) Warren M, Guha PK, Berenfeld O, Zaitsev A, Anumonwo JM, Dhamoon AS, Bagwe S, Taffet SM, Jalife J : Blockade of the inward rectifying potassium current terminates ventricular fibrillation in the guinea pig heart. J Cardiovasc Electrophysiol. 2003 ; 14 : 621～631
29) Noujaim SF, Pandit SV, Berenfeld O, Vikstrom K, Cerrone M, Mironov S, Zugermayr M, Lopatin AN, Jalife J : Up-regulation of the inward rectifier K+current (IK1) in the mouse heart accelerates and stabillizes rotors. J Physiol. 2007 ; 578 : 315～326
30) Chen PS, Wu TJ, Ting CT, Karagueuzian HS, Garfinkel A, Lin SF, Weiss JN : A tale of two fibrillation. Circulation. 2003 ; 108 : 2298～2303
31) Ripplinger CM, KrinskyVI, Nikolski VP, Efimov IR : Mechanisms of unpinning and termination of ventricular tachycardia. Am J Physiol Heart Circ Physiol. 2006 ; 291 : H184～H192
32) Gray RA, Chattipakorn N : Termination of spiral waves during cardiac fibrillation via shock-induced phase resetting. PNAS. 2005 ; 102 : 4672～4677
33) Efimov IR, Cheng Y, Van Vagoner DR, Mazgalev T, Tchou PJ : Virtual electrode-induced phase singularity. A basic mechanism of defibrillation failure. Circ Res. 1998 ; 82 : 918～925
34) Dorian P, Penkoske PA, Witkowski FX : Order in disorder : effect of barium on ventricular fibrillation. Can J Cardiol. 1996 ; 12 : 399～406
35) Dorian P, Cass D : An overview of the management of electrical storm. Can J Cardiol. 1997 ; 13 (Suppl A) : 13A～17A

Pressor response induced by central angiotensin II is mediated by activation of Rho/Rho-kinase pathway via AT_1 receptors

Yoji Sagara, Yoshitaka Hirooka, Masatsugu Nozoe, Koji Ito, Yoshikuni Kimura and Kenji Sunagawa

Objectives **The brain renin–angiotensin system plays an important role in cardiovascular regulation and the pathogenesis of hypertension. Angiotensin II activates the Rho/Rho-kinase pathway in vascular smooth muscle cells and cardiomyocytes *in vitro*. The aim of the present study was to determine whether angiotensin II in the brainstem activates the Rho/Rho-kinase pathway, and, if so, whether this mechanism is involved in the central pressor action of angiotensin II.**

Methods and results **Angiotensin II infused intracisternally for 7 days in Wistar–Kyoto rats (WKY) increased systolic blood pressure (SBP) and urinary norepinephrine excretion. These responses were abolished by the co-infusion of Y-27632, a specific Rho-kinase inhibitor, or valsartan. The intracisternal infusion of Y-27632 or valsartan also reduced SBP and norepinephrine excretion in spontaneously hypertensive rats (SHR). Western blot analysis was performed to examine the expression levels of membranous RhoA and phosphorylated ezrin, radixin, and moesin (p-ERM), which reflects Rho/Rho-kinase activity. The expression levels of membranous RhoA and p-ERM in the brainstem were significantly greater in both angiotensin II-treated WKY and SHR than in vehicle-treated WKY. Valsartan reduced the expression levels of membranous RhoA and p-ERM in angiotensin II-treated WKY and SHR. Y-27632 reduced the expression levels of p-ERM in angiotensin II-treated WKY and SHR.**

Conclusions **These results suggest that the pressor response induced by intracisternally infused angiotensin II is substantially mediated by the activation of the Rho/Rho-kinase pathway via AT_1 receptors of the brainstem in WKY, and that this pathway might be involved in the hypertensive mechanisms of SHR. *J Hypertens* 25:399–406 © 2007 Lippincott Williams & Wilkins.**

Journal of Hypertension 2007, 25:399–406

Keywords: angiotensin II, blood pressure, brain, Rho, sympathetic nervous system

Department of Cardiovascular Medicine, Kyushu University Graduate School of Medical Sciences, Fukuoka, Japan

Correspondence and requests for reprints to Yoshitaka Hirooka, Department of Cardiovascular Medicine, Kyushu University Graduate School of Medical Sciences, 3-1-1 Maidashi, Higashi-ku, Fukuoka 812-8582, Japan
Tel: +81 92 642 5360; fax: +81 92 642 5374;
e-mail: hyoshi@cardiol.med.kyushu-u.ac.jp

Sponsorship: This study was supported by grants-in-aid for Scientific Research from the Japan Promotion of Science (S18659230, C17590745).

Conflict of interest: none.

Received 18 May 2006 **Revised** 15 August 2006
Accepted 11 September 2006

Introduction

Angiotensin II is critical for the regulation of vascular tone, blood pressure, and volume homeostasis. The physiological actions of angiotensin II occur through its binding to two main cell surface receptors, AT_1 and AT_2. The cardiovascular effects of angiotensin II are widely considered to result from AT_1 receptor activation. The brain renin–angiotensin system is also considered pivotal in cardiovascular regulation and is important in the pathogenesis of hypertension [1,2]. The specific mechanisms by which increased brain renin–angiotensin system activity results in hypertension are not well understood, but include increased sympathetic vasomotor tone and impaired arterial baroreflex function.

The involvement of the small guanosine triphosphatase Rho and its downstream effector Rho-kinase [3] is implicated in various cellular functions, including actin cytoskeleton organization [4], cell adhesion and motility [5,6], myosin light chain phosphorylation, and smooth muscle contraction [7]. Y-27632, a specific Rho-kinase inhibitor [8,9], dramatically reduces hypertension in rat hypertension models [9]. In addition, Rho-kinase activity is increased in hypertensive blood vessels [10], and the inhibition of Rho-kinase induces preferential forearm vasodilation in hypertensive patients [11]. Activation of the Rho/Rho-kinase pathway thus contributes to the pathophysiology of hypertension [9–11]. Recent results indicate that the Rho/Rho-kinase pathway is involved in AT_1 receptor signaling. The Rho/Rho-kinase pathway is activated in angiotensin II-induced hypertrophy of vascular smooth muscle cells and cardiomyocytes [12,13]. RhoA and Rho-kinase are also found in the central nervous system [14,15]. Rho/Rho-kinase is present in the nucleus of the solitary tract (NTS) in the brainstem, and activation of the Rho/Rho-kinase pathway in the

NTS contributes to the neural mechanisms of hypertension in spontaneously hypertensive rats (SHR) and in a hypertensive rat model of chronic nitric oxide synthase inhibition [16,17]. Furthermore, inhibition of this pathway in the NTS augments baroreflex control of the heart rate and enhances glutamate sensitivity in SHR [18,19]. It remains to be determined, however, whether activation of the Rho/Rho-kinase pathway also contributes to neurogenic hypertensive mechanisms caused by angiotensin II. The aim of the present study was to elucidate the role of the Rho/Rho-kinase pathway in the brainstem on the central effects of angiotensin II. For this purpose, we infused angiotensin II intracisternally for 7 days with a mini-osmotic pump in Wistar–Kyoto rats (WKY). Then, Y-27632 or valsartan was infused intracisternally in angiotensin II-treated WKY or SHR. Systolic blood pressure (SBP) and heart rate were measured using the tail-cuff method. Urinary norepinephrine excretion was measured as a marker of sympathetic nerve activity. Finally, we evaluated RhoA and Rho-kinase activity in the brainstem by western blot analysis.

Methods

This study was reviewed and approved by the Committee on Ethics of Animal Experiments, Kyushu University Graduate School of Medical Sciences, and was conducted according to the Guidelines for Animal Experiments of Kyushu University. Male WKY or SHR (280–340 g, 16–20 weeks old) were used in the present study. Rats were obtained from an established colony at the Animal Research Institute of Kyushu University Faculty of Medicine (Fukuoka, Japan) [16,17].

Continuous infusion experiments with angiotensin II, Y-27632, valsartan, and phenylephrine

Angiotensin II (0.1 mg/kg per day) or vehicle (artificial cerebrospinal fluid) were infused intracisternally (0.25 μl/h) for 7 days with a mini-osmotic pump (Alzet model 1002; Durect Corporation, Cupertino, California, USA) in WKY. Y-27632 (5 or 10 mmol/l) or valsartan (0.5 mg/kg per day) were infused intracisternally (0.25 μl/h) in angiotensin II-treated WKY or SHR. The rats were anaesthetized with sodium pentobarbital (50 mg/kg, intraperitoneally). The mini-osmotic pump, filled with angiotensin II, vehicle, Y-27632, or valsartan was implanted subcutaneously in the back and connected to a polyethylene tube (PE10). A small hole was then made in the atlanto-occipital membrane, which covers the dorsal surface of the medulla, and the tip of the tube was placed intracisternally and fixed in place with tissue adhesive. At the end of the infusion, we confirmed intracisternal delivery of drug in each rat by checking the connection of the tube and the placement of its tip. Phenylephrine (1 mg/kg per day) was infused subcutaneously for 7 days using a mini-osmotic pump (Alzet model 2001; Durect Corporation) in WKY. After full recovery from anaesthesia, the rats were free to move about in their cages.

Measurement of blood pressure, heart rate, and urinary norepinephrine excretion

SBP and heart rate were measured using the tail-cuff method before and during treatment. We measured SBP and heart rate blinded to the group membership of the rats. We collected urine for 24 h using a metabolic cage. We measured the urinary norepinephrine concentration by high-performance liquid chromatography before and at day 7, and calculated the urinary norepinephrine excretion for 24 h, as described previously [20].

Western blot analysis

We performed western blot analysis for phosphorylated ezrin, radixin, and moesin (p-ERM) or total ezrin, radixin, and moesin family members (ezrin, radixin, and moesin), which are target proteins of Rho-kinase [21] and membranous or total RhoA (1 : 1000; Santa Cruz Biotechnology, Santa Cruz, California, USA), in the brainstem (a coronal section; 3 mm caudal to 2 mm rostral to the obex), as described previously [16].

Statistical analysis

All values are expressed as means ± SEM. Two-way analysis of variance was used to compare SBP and heart rate between any two groups. Comparisons between any two mean values were performed using Bonferroni's correction for multiple comparisons. A paired *t*-test was used to compare 24-h urinary norepinephrine excretion before and at day 7 during treatment. Differences were considered to be statistically significant when $P < 0.05$.

Results

Intracisternal infusion of angiotensin II and co-infusion of Y-27632 or valsartan in Wistar–Kyoto rats

Figure 1a shows the time course of SBP and heart rate after the intracisternal infusion of angiotensin II or vehicle in WKY. SBP was significantly increased in angiotensin II-treated rats compared with vehicle-treated rats. The co-infusion of Y-27632 (5 mmol/l) or valsartan significantly attenuated the increase in SBP induced by angiotensin II. There were no significant differences in heart rate between any two groups. The intracisternal infusion of angiotensin II significantly increased urinary norepinephrine excretion. This response was abolished by the co-infusion of Y-27632 or valsartan (Fig. 1b).

Effect of angiotensin II on Rho/Rho-kinase activity in the brainstem

To confirm the effects of the intracisternal infusion of angiotensin II on Rho/Rho-kinase activity in the brainstem, we examined the expression levels of membranous RhoA, which represent RhoA activity, and the expression levels of p-ERM, which represent Rho-kinase activity. The expression levels of membranous RhoA in the

Fig. 1

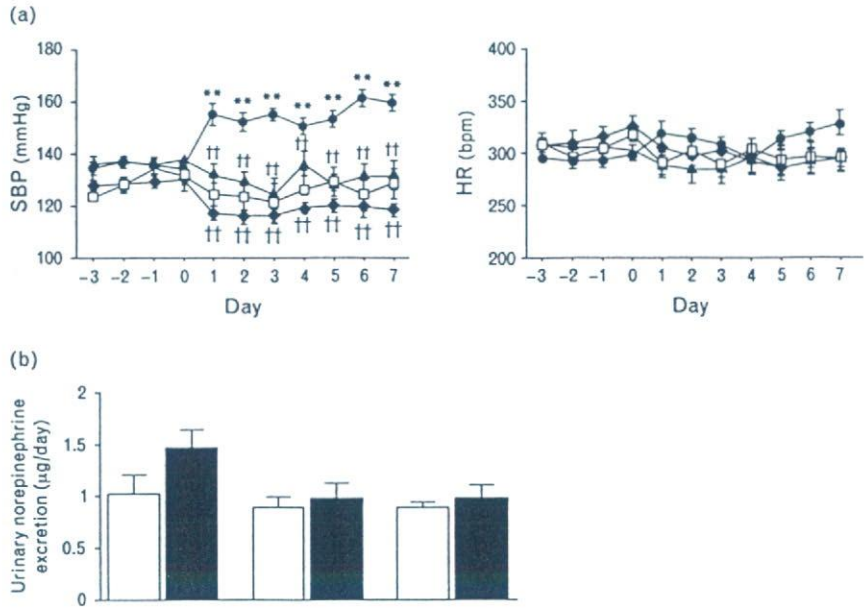

(a) Time course of systolic blood pressure (SBP) and heart rate (HR) before and during the intracisternal infusion of vehicle, angiotensin II (AngII), co-infusion of angiotensin II and Y-27632, or co-infusion of angiotensin II and valsartan ($n = 10$ for each). $^{**}P < 0.01$ compared with the vehicle group; $^{\dagger\dagger}P < 0.01$ compared with the angiotensin II group. □ Vehicle; ● AngII; ▲ AngII and Y-27632; ◆ AngII and valsartan. (b) Urinary norepinephrine excretion before and at day 7 during the intracisternal infusion of angiotensin II, co-infusion of angiotensin II and Y-27632, or co-infusion of angiotensin II and valsartan ($n = 6$ per group). $^{*}P < 0.05$ compared with pretreatment values. □ Before; ■ after.

brainstem were greater in angiotensin II-treated rats than in vehicle-treated rats (Fig. 2a). Furthermore, the expression levels of p-ERM in the brainstem were greater in angiotensin II-treated rats than in vehicle-treated rats (Fig. 2b).

Inhibitory effects of Y-27632 or valsartan on Rho/Rho-kinase activation by angiotensin II

Valsartan significantly reduced the expression levels of membranous RhoA in angiotensin II-treated rats (Fig. 2a). In addition, Y-27632 or valsartan significantly reduced the

Fig. 2

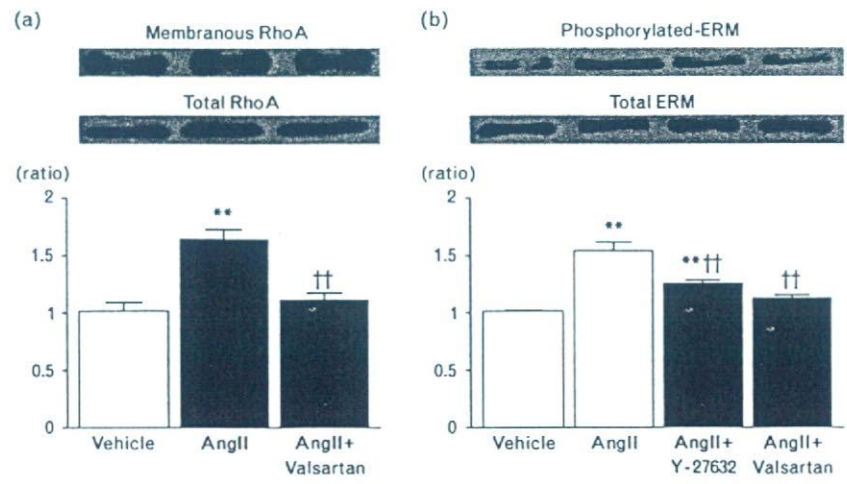

(a) Expression levels of membranous RhoA and total RhoA evaluated by Western blot analysis during the intracisternal infusion of vehicle, angiotensin II (AngII), or co-infusion of angiotensin II and valsartan ($n = 5$ for each). The graph shows the ratio of membranous RhoA to total RhoA. (b) Expression levels of phosphorylated ezrin, radixin, and moesin (ERM) and total ERM evaluated by western blot analysis during the intracisternal infusion of vehicle, angiotensin II ($n = 10$ for each), co-infusion of angiotensin II and Y-27632, or co-infusion of angiotensin II and valsartan ($n = 8$ for each). The graph shows the ratio of p-ERM to total ERM. Data are expressed as the relative ratio to vehicle, which was assigned a value of 1. $^{**}P < 0.01$ compared with the vehicle group; $^{\dagger\dagger}P < 0.01$ compared with the angiotensin II group.

expression levels of p-ERM in angiotensin II-treated rats (Fig. 2b).

Effect of subcutaneous infusion of phenylephrine on Rho/Rho-kinase activity

To examine whether activation of the Rho/Rho-kinase pathway in the brainstem was caused by the pressure response, phenylephrine was infused subcutaneously in WKY. The subcutaneous infusion of phenylephrine increased SBP to the same level as the intracisternal infusion of angiotensin II (Fig. 3a). The subcutaneous infusion of phenylephrine, however, did not alter the expression levels of membranous RhoA and p-ERM in the brainstem (Fig. 3b).

Intracisternal infusion of Y-27632 or valsartan in spontaneously hypertensive rats

The intracisternal infusion of Y-27632 (10 mmol/l) or valsartan significantly reduced SBP and heart rate in SHR (Fig. 4a). Urinary norepinephrine excretion was significantly higher in SHR than in WKY. Furthermore, the intracisternal infusion of Y-27632 or valsartan significantly reduced urinary norepinephrine excretion in SHR (Fig. 4b).

Rho/Rho-kinase activity in the brainstem of spontaneously hypertensive rats

The expression levels of membranous RhoA in the brainstem were greater in vehicle-treated SHR than in vehicle-treated WKY. The intracisternal infusion of valsartan reduced the expression levels of membranous RhoA in SHR (Fig. 5a). Furthermore, the expression levels of p-ERM in the brainstem were greater in vehicle-treated SHR than in vehicle-treated WKY. The intracisternal infusion of Y-27632 or valsartan reduced the expression levels of p-ERM in SHR (Fig. 5b).

Effect of central AT_1 receptor blockade in Wistar–Kyoto and spontaneously hypertensive rats

The intracisternal infusion of valsartan reduced SBP in WKY. The magnitude of the decrease, however, was significantly higher in SHR (210 ± 2 to 182 ± 5 mmHg) than in WKY (122 ± 6 to 110 ± 3 mmHg). The intracisternal infusion of valsartan significantly reduced heart rate in SHR (346 ± 10 to 316 ± 14 bpm), but not in WKY (317 ± 16 to 310 ± 10 bpm; Fig. 6).

Fig. 3

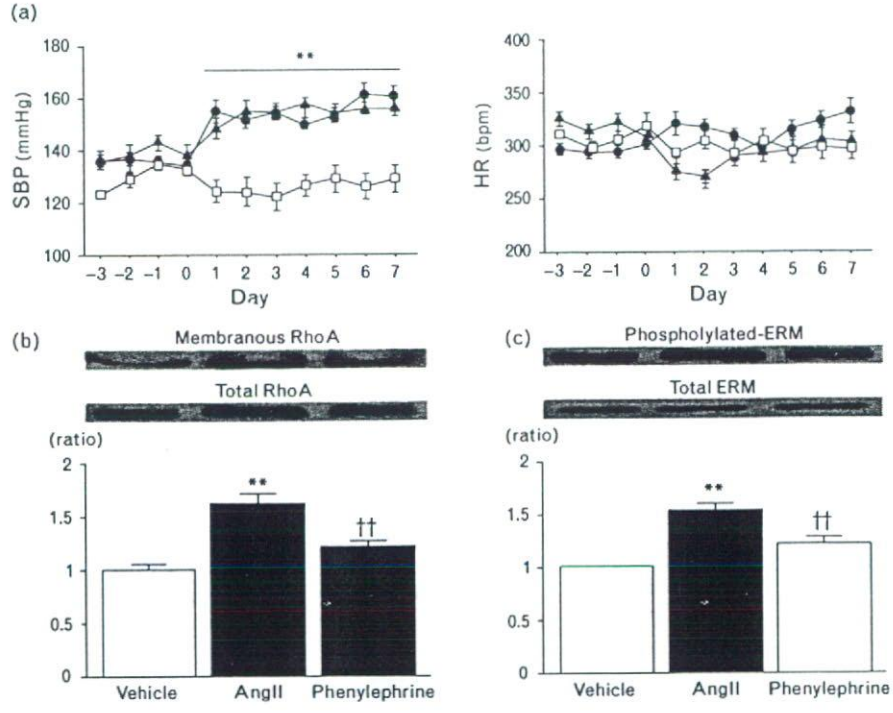

(a) Time course of systolic blood pressure (SBP) and heart rate (HR) before and during the intracisternal infusion of vehicle, angiotensin II, or subcutaneous infusion of phenylephrine ($n = 10$ for each). □ Vehicle; ● angiotensin II; ▲ phenylephrine. (b) Expression levels of membranous RhoA and total RhoA evaluated by Western blot analysis during the intracisternal infusion of vehicle, angiotensin II, or subcutaneous infusion of phenylephrine ($n = 5$ for each). The graph shows the ratio of membranous RhoA to total RhoA. Data are expressed as the relative ratio to vehicle, which was assigned a value of 1. (c) Expression levels of phosphorylated ezrin, radixin, and moesin (ERM) and total ERM evaluated by western blot analysis during the intracisternal infusion of vehicle, angiotensin II, or subcutaneous infusion of phenylephrine ($n = 10$ for each). The graph shows the ratio of p-ERM to total ERM. Data are expressed as the relative ratio to vehicle, which was assigned a value of 1. The results of vehicle and angiotensin II infusion are obtained from Fig. 1 and Fig. 2 for comparison. $^{**}P < 0.01$ compared with the vehicle group; $^{\dagger\dagger}P < 0.01$ compared with the angiotensin II group.

Fig. 4

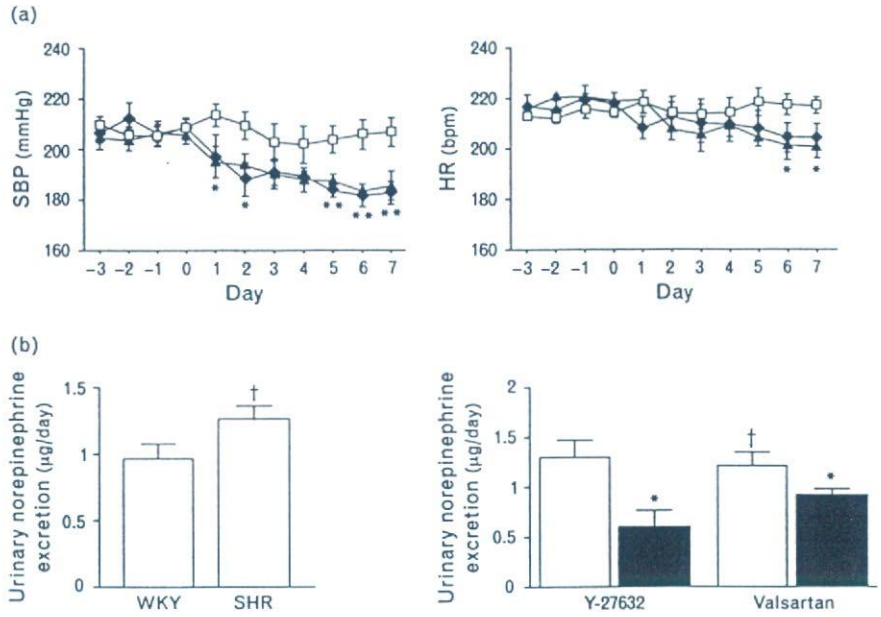

(a) Time course of systolic blood pressure (SBP) and heart rate (HR) before and during the intracisternal infusion of vehicle, Y-27632, or valsartan in SHR ($n=5$ for each). $^{*}P<0.05$; $^{**}P<0.01$ compared with the vehicle group, respectively. □ Vehicle; ▲ Y-27632; ◆ valsartan. (b) Urinary norepinephrine excretion in Wistar–Kyoto rats (WKY) and spontaneously hypertensive rats (SHR) ($n=5$ for each; left), and before and at day 7 during the intracisternal infusion of Y-27632 or valsartan in SHR ($n=5$ per group; right). $^{\dagger}P<0.05$ compared with the values of WKY; $^{*}P<0.05$ compared with pretreatment values. □ Before; ■ after.

Discussion

In the present study, pressor and sympathoexcitatory responses evoked by the intracisternal infusion of angiotensin II were abolished by the co-infusion of Y-27632 in WKY. The effects of angiotensin II on these responses were mediated by AT_1 receptors, because valsartan

Fig. 5

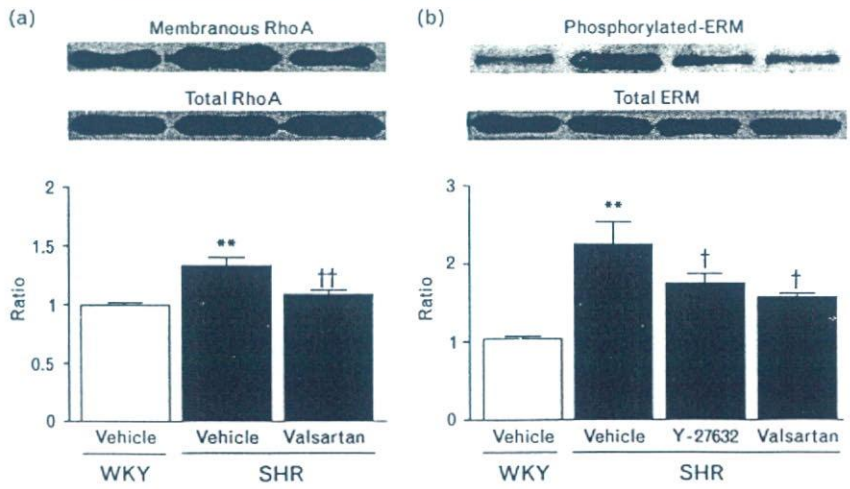

(a) Expression levels of membranous RhoA and total RhoA evaluated by western blot analysis in Wistar–Kyoto rats (WKY; vehicle) and spontaneously hypertensive rats (SHR; during the intracisternal infusion of vehicle or valsartan; $n=5$ for each). The graph shows the ratio of membranous RhoA to total RhoA. (b) Expression levels of p-ERM and total ERM evaluated by western blot analysis in WKY (vehicle) and SHR (during the intracisternal infusion of vehicle, Y-27632, or valsartan; $n=5$ for each). The graph shows the ratio of p-ERM to total ERM. Data are expressed as the relative ratio to WKY, which was assigned a value of 1. $^{**}P<0.01$ compared with the WKY group; $^{\dagger}P<0.05$; $^{\dagger\dagger}P<0.01$ compared with the vehicle-treated SHR group, respectively.

Fig. 6

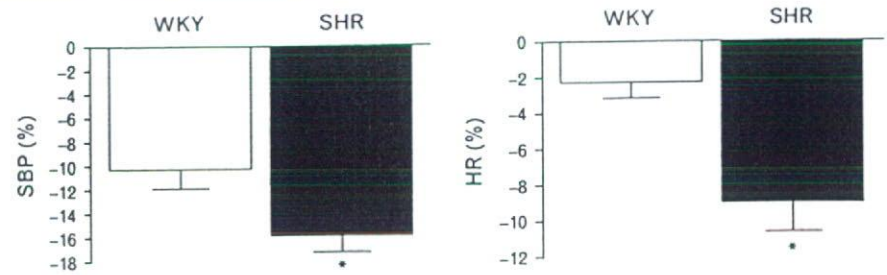

Changes in systolic blood pressure (SBP) and heart rate (HR) at day 7 during the intracisternal infusion of valsartan in Wistar–Kyoto rats (WKY) and spontaneously hypertensive rats (SHR; $n = 5$ for each). Data are expressed as the relative ratio to day 0, which was assigned a value of 100%. *$P < 0.05$ compared with the WKY group.

blocked the responses. The expression level of membranous RhoA represents RhoA activity [22]. The expression was significantly increased by the intracisternal infusion of angiotensin II and blocked by the co-infusion of valsartan in WKY. The expression level of p-ERM represents Rho-kinase activity and was also significantly increased by the intracisternal infusion of angiotensin II in WKY. This response was blocked by the co-infusion of either valsartan or Y-27632. Furthermore, the intracisternal infusion of Y-27632 reduced SBP and urinary norepinephrine excretion in SHR. Y-27632 reduced the expression levels of p-ERM in the brainstem of SHR. Valsartan reduced the expression levels of both membranous RhoA and p-ERM. Taken together, these results suggest that exogenous angiotensin II applied to the brainstem activates the brain Rho/Rho-kinase pathway, as in the aorta and heart [12,13], and thereby increases SBP through the sympathetic nervous system via AT_1 receptors in WKY. Moreover, the inhibition of endogenous AT_1 receptors in the brainstem reduces increased RhoA and Rho-kinase activity in SHR, thereby at least partly inhibiting SBP in SHR.

The brain renin–angiotensin system is closely associated with blood pressure regulation via the sympathetic nervous system, although it is also related to other physiological responses, such as drinking behaviour via the vasopressin system [23]. Although vasopressin might be involved in the pressor response to the intracisternal infusion of angiotensin II [24], resetting of the arterial baroreflex towards higher pressures occurs with the long-term infusion of angiotensin II, and this resetting permits high sympathetic nerve activity [25]. Our results are consistent with these previously reported findings, indicating that centrally administered angiotensin II elicits pressor and sympathoexcitatory responses via activation of the Rho/Rho-kinase pathway in WKY. Furthermore, activation of the brain renin–angiotensin system is one of the hypertensive mechanisms in animal models of hypertension [26,27]. Angiotensin immunoreactivity [28] and AT_1 receptor expression levels [29] are greater in the brainstem of SHR than WKY. Whereas there is some evidence that the brain renin–angiotensin system is not an important factor in causing hypertension [30,31], we demonstrated that the intracisternal infusion of valsartan reduced SBP and heart rate to a greater extent in SHR than in WKY. This result suggests that the endogenous brain renin–angiotensin system is activated in SHR.

The sites of action of the intracisternal infusion of angiotensin II are not clear from the results of the present study. AT_1 receptors appear to dominate in cardiovascular control regions [32], however, and many nuclei in these regions are activated by the central infusion of angiotensin II, as evaluated by c-*fos* expression, which is a marker of neuronal excitation [33]. The NTS and rostral ventrolateral medulla are possible candidates. The microinjection of angiotensin II into the NTS [34] or rostral ventrolateral medulla [35] elicits pressor and sympathoexcitatory responses. This is particularly apparent in animal models of hypertension [36,37]. Although some studies have indicated that the microinjection of angiotensin II into the NTS produces a depressor effect [38], the response to the microinjection of angiotensin II into the NTS exhibits a complicated dose–response relationship [39]. We previously reported that the microinjection of Y-27632 into the NTS decreases blood pressure in SHR and nitro-L-arginine methyl ester-treated rats [16,17], in which the endogenous renin–angiotensin system is activated. Although we did not specifically examine the NTS in the present study, activation of the Rho/Rho-kinase pathway in the NTS by angiotensin II might contribute, at least partly, to the increase in blood pressure.

Activation of the Rho/Rho-kinase pathway in the brainstem is not caused by the pressor response *per se*, because the subcutaneous infusion of phenylephrine does not activate this pathway. It is possible that the pressor response was centrally elicited by other substances, such as *N*-methyl-D-aspartate or an α_2 antagonist, which are not considered to be related to the Rho/Rho-kinase

pathway, but might also activate this pathway. Further studies are needed to clarify this issue.

Activation of AT_1 receptors also alters signaling pathways other than the Rho/Rho-kinase pathway, such as the mitogen-activated protein kinase and nicotinamide adenine dinucleotide phosphate, reduced form oxidase pathways [40,41]. Nicotinamide adenine dinucleotide phosphate, reduced form oxidase pathways stimulates another Rho family member, rac1 [42], which enhances superoxide anion generation [43]. Interaction between Rho and other Rho family members such as rac1 or cdc42 have been reported *in vitro* [44]. The type of physiological response involved in their interaction *in vivo*, however, remains unknown. There are some studies that do not support an antihypertensive effect of Y-27632. Y-27632 (3 mg/kg per day) did not affect SBP in Dahl salt-sensitive hypertensive rats [45]. In nitro-L-arginine methyl ester-treated rats, however, Y-27632 (30 mg/kg per day) reduces blood pressure, whereas lower doses of Y-27632 (10 mg/kg per day) do not affect blood pressure [46]. Therefore, Y-27632 appears to have a dose-dependent antihypertensive effect, although we cannot exclude the possibility that activation of the Rho/Rho-kinase pathway differs among the hypertensive models.

The precise mechanism(s) by which angiotensin II activates RhoA and Rho-kinase is unknown, particularly in the brain. Rho-kinase plays an important role in angiotensin II-induced messenger RNA expression of monocyte chemoattractant protein 1, transforming growth factor 1, and plasminogen activator inhibitor 1 [46–48]. In cultured human coronary vascular smooth muscle cells, the expression of Rho-kinase is enhanced by inflammatory stimuli, such as angiotensin II and IL-1 [49]. Complex signal transduction pathways might thus be involved in producing the final physiological responses.

In conclusion, the results of the present study suggest that centrally administered angiotensin II activates the Rho/Rho-kinase pathway in the brainstem nuclei, thereby increasing central sympathetic outflow and blood pressure. In addition, it is possible that inhibition of endogenous Rho-kinase in the brainstem decreases central sympathetic outflow, thereby decreasing blood pressure in SHR.

References

1 Bunnemann B, Fuxe K, Ganten D. The brain reninangiotensin system: localization and general significance. *J Cardiovasc Pharmacol* 1992; **19 (Suppl. 6)**:51–62.

2 Phillips MI. Functions of angiotensin in the central nervous system. *Annu Rev Physiol* 1987; **49**:413–435.

3 Matsui T, Amano M, Yamamoto T, Chihara K, Nakafuku M, Ito M, *et al.* Rho-associated kinase, a novel serine/threonine kinase, as a putative target for the small GTP binding protein Rho. *EMBO J* 1996; **15**:2208–2216.

4 Hall A. Rho GTPases and the actin cytoskeleton. *Science* 1998; **279**:509–514.

5 Ridley AJ, Hall A. The small GTP-binding protein Rho regulates the assembly of focal adhesions and actin stress fibers in response to growth factors. *Cell* 1992; **70**:389–399.

6 Horwitz AR, Parsons JT. Cell migration: movin' on. *Science* 1999; **286**:1102–1103.

7 Kureishi Y, Kobayashi S, Amano M, Kimura K, Kanaide H, Nakano T, *et al.* Rho-associated kinase directly induces smooth muscle contraction through myosin light chain phosphorylation. *J Biol Chem* 1997; **272**:12257–12260.

8 Ishizaki T, Uehata M, Tamechika I, Keel J, Nonomura K, Maekawa M, *et al.* Pharmacological properties of Y-27632, a specific inhibitor of Rho-associated kinases. *Mol Pharmacol* 2000; **57**:976–983.

9 Uehata M, Ishizaki T, Satoh H, Ono T, Kawahara T, Morishita T, *et al.* Calcium sensitization of smooth muscle mediated by a Rho-associated protein kinase in hypertension. *Nature* 1997; **389**:990–994.

10 Mukai Y, Shimokawa H, Matoba T, Kandabashi T, Satoh S, Hiroki J, *et al.* Involvement of Rho-kinase in hypertensive vascular disease: a novel therapeutic target in hypertension. *FASEB J* 2001; **15**:1062–1064.

11 Masumoto A, Hirooka Y, Shimokawa H, Hironaga K, Setoguchi S, Takeshita A. Possible involvement of Rho-kinase in the pathogenesis of hypertension in humans. *Hypertension* 2001; **38**:1307–1310.

12 Yamakawa T, Tanaka S, Numaguchi K, Yamakawa Y, Motley ED, Ichihara S, Inagami T. Involvement of Rho-kinase in angiotensin II-induced hypertrophy of rat vascular smooth muscle cells. *Hypertension* 2000; **35**:313–318.

13 Aoki H, Izumo S, Sadoshima J. Angiotensin II activates RhoA in cardiac myocytes: a critical role of RhoA in angiotensin II-induced premyofibril formation. *Circ Res* 1998; **82**:666–676.

14 Hashimoto R, Nakamura Y, Kosako H, Amano M, Kaibuchi K, Inagaki M, Takeda M. Distribution of Rho-kinase in the bovine brain. *Biochem Biophys Res Commun* 1999; **263**:575–579.

15 Olenik C, Barth H, Just I, Aktories K, Meyer DK. Gene expression of the small GTP-binding proteins RhoA, RhoB, Rac1, and Cdc42 in adult rat brain. *Mol Brain Res* 1997; **52**:263–269.

16 Ito K, Hirooka Y, Sakai K, Kishi T, Kaibuchi K, Shimokawa H, Takeshita A. Rho/Rho-kinase pathway in brain stem contributes to blood pressure regulation via sympathetic nervous system: possible involvement in neural mechanisms of hypertension. *Circ Res* 2003; **92**:1337–1343.

17 Ito K, Hirooka Y, Kishi T, Kimura Y, Kaibuchi K, Shimokawa H, Takeshita A. Rho/Rho-kinase pathway in the brainstem contributes to hypertension caused by chronic nitric oxide synthase inhibition. *Hypertension* 2004; **43**:156–162.

18 Ito K, Hirooka Y, Sagara Y, Kimura Y, Kaibuchi K, Shimokawa H, *et al.* Inhibition of Rho-kinase in the brainstem augments baroreflex control of heart rate in rats. *Hypertension* 2004; **44**:478–483.

19 Ito K, Hirooka Y, Hori N, Kimura Y, Sagara Y, Shimokawa H, *et al.* Inhibition of Rho-kinase in the nucleus tractus solitarius enhances glutamate sensitivity in rats. *Hypertension* 2005; **46**:360–365.

20 Sakai K, Hirooka Y, Matsuo I, Eshima K, Shigematsu H, Shimokawa H, Takeshita A. Overexpression of eNOS in NTS causes hypotension and bradycardia in vivo. *Hypertension* 2000; **36**:1023–1028.

21 Matsui T, Maeda M, Doi Y, Yonemura S, Amano M, Kaibuchi K, Tsukita S. Rho-kinase phosphorylate COOH-terminal threonines of ezrin/radixin/moesin (ERM) proteins and regulates their head-to-tail association. *J Cell Biol* 1998; **140**:647–657.

22 Liao JK, Homcy CJ. Specific receptor-guanine nucleotide binding protein interaction mediates the release of endothelium-derived relaxing factor. *Circ Res* 1992; **70**:1018–1026.

23 Steckelings U, Lebrun C, Qadri F, Veltmar A, Unger T. Role of brain angiotensin in cardiovascular regulation. *J Cardiovasc Pharmacol* 1992; **19**:72–79.

24 Sun MK, Reis DJ. Intracisternally applied angiotensin II does not excite reticulospinal vasomotor neurons in anesthetized rats. *Eur J Pharmacol* 1996; **304**:63–71.

25 Bishop VS, Ryuzaki M, Cai Y, Nishida Y, Cox BF. Angiotensin II-dependent hypertension and the arterial baroreflex. *Clin Exp Hypertens* 1995; **17**:29–38.

26 Ruiz P, Basso N, Cannata MA, Taquini AC. The renin–angiotensin system in different stages of spontaneous hypertension in the rat (SHR). *Clin Exp Hypertens* 1990; **12**:63–81.

27 Phillips MI, Kimura B. Brain angiotensin in the developing spontaneously hypertensive rat. *J Hypertens* 1988; **6**:607–612.

28 Meyer JM, Felten DL, Weyhenmeyer JA. Levels of immunoreactive angiotensin II in microdissected nuclei from adult WKY and SH rat brain. *Clin Exp Hypertens* 1989; **11**:103–117.

29 Song K, Kurobe Y, Kanehara H, Okunishi H, Wada T, Inada Y, *et al.* Quantitative localization of angiotensin II receptor subtypes in spontaneously hypertensive rats. *Blood Press* 1994; **5 (Suppl.)**:21–26.

30 Paull JR, Bunting MW, Widdop RE. Role of the brain renin–angiotensin system in the maintenance of blood pressure in conscious spontaneously hypertensive and sinoaortic baroreceptor-denervated rats. *Clin Exp Pharmacol Physiol* 1997; **24**:667–672.

31 Bunting MW, Widdop RE. Lack of a centrally-mediated antihypertensive effect following acute or chronic central treatment with AT1-receptor antagonists in spontaneously hypertensive rats. *Br J Pharmacol* 1995; **116**:3181–3190.

32 McKinley MJ, McAllen RM, Pennington GL, Smardencas A, Weisinger RS, Oldfield BJ. Physiological actions of angiotensin II mediated by AT1 and AT2 receptors in the brain. *Clin Exp Pharmacol Physiol* 1996; **3 (Suppl.)**:99–104.

33 Hirooka Y, Head GA, Potts PD, Godwin SJ, Bendle RD, Dampney RAL. Medullary neurons activated by angiotensin II in conscious rabbit. *Hypertension* 1996; **27**:287–296.

34 Casto R, Phillips MI. Mechanism of pressor effects by angiotensin in the nucleus tractus solitarius of rats. *Am J Physiol* 1984; **247**:575–581.

35 Averill DB, Tsuchihashi T, Khosla MC, Ferrario CM. Losartan, nonpeptide angiotensin II-type 1 (AT1) receptor antagonist, attenuates pressor and sympathoexcitatory responses evoked by angiotensin II and L-glutamate in rostral ventrolateral medulla. *Brain Res* 1994; **665**:245–252.

36 Casto R, Phillips MI. Neuropeptide action in nucleus tractus solitarius: angiotensin specificity and hypertensive rats. *Am J Physiol* 1985; **249**:341–347.

37 Muratani H, Ferrario CM, Averill DB. Ventrolateral medulla in spontaneously hypertensive rats: role of angiotensin II. *Am J Physiol Regul Integr Comp Physiol* 1993; **264**:388–395.

38 Barnes KL, DeWeese DM, Andresen MC. Angiotensin potentiates excitatory sensory synaptic transmission to medial solitary tract nucleus neurons. *Am J Physiol Regul Integr Comp Physiol* 2003; **284**:1340–1353.

39 Rettig R, Healy DP, Printz MP. Cardiovascular effects of microinjections of angiotensin II into the nucleus tractus solitarii. *Brain Res* 1986; **364**:233–240.

40 Yang H, Raizada MK. MAP kinase-independent signaling in angiotensin II regulation of neuromodulation in SHR neurons. *Hypertension* 1998; **32**:473–481.

41 Griendling KK, Minieri CA, Ollerenshaw JD, Alexander RW. Angiotensin II stimulates NADH and NADPH oxidase activity in cultured vascular smooth muscle cells. *Circ Res* 1994; **74**:1141–1148.

42 Bokoch GM, Diebold BA. Current molecular models for NADPH oxidase regulation by Rac GTPase. *Blood* 2002; **100**:2692–2696.

43 Gregg D, Rauscher FM, Goldschmidt-Clermont PJ. Rac regulates cardiovascular superoxide through diverse molecular interactions: more than a binary GTP switch. *Am J Physiol Cell Physiol* 2003; **285**:723–734.

44 Yuan XB, Jin M, Xu X, Song YQ, Wu CP, Poo MM, Duan S. Signalling and crosstalk of Rho GTPases in mediating axon guidance. *Nat Cell Biol* 2003; **5**:38–45.

45 Mita S, Kobayashi N, Yoshida K, Nakano S, Matsuoka H. Cardioprotective mechanisms of Rho-kinase inhibition associated with eNOS and oxidative stress-LOX-1 pathway in Dahl salt-sensitive hypertensive rats. *J Hypertens* 2005; **23**:87–96.

46 Kataoka C, Egashira K, Inoue S, Takemoto M, Ni W, Koyanagi M, *et al.* Important role of Rho-kinase in the pathogenesis of cardiovascular inflammation and remodeling induced by long-term blockade of nitric oxide synthesis in rats. *Hypertension* 2002; **39**:245–250.

47 Funakoshi Y, Ichiki T, Shimokawa H, Egashira K, Takeda K, Kaibuchi K, *et al.* Rho-kinase mediates angiotensin II-induced monocyte chemoattractant protein-1 expression in rat vascular smooth muscle cells. *Hypertension* 2001; **38**:100–104.

48 Takeda K, Ichiki T, Tokunou T, Iino N, Fujii S, Kitabatake A, *et al.* Critical role of Rho-kinase and MEK/ERK pathways for angiotensin II-induced plasminogen activator inhibitor type-1 gene expression. *Arterioscler Thromb Vasc Biol* 2001; **21**:868–873.

49 Hiroki J, Shimokawa H, Higashi M, Morikawa K, Kandabashi T, Kawamura N, *et al.* Inflammatory stimuli upregulate Rho-kinase in human coronary vascular smooth muscle cells. *J Mol Cell Cardiol* 2004; **37**:537–546.

Percutaneous Coronary Arterial Thrombectomy for Acute Myocardial Infarction Reduces No-Reflow Phenomenon and Protects Against Left Ventricular Remodeling Related to the Proximal Left Anterior Descending and Right Coronary Artery

Takuya KISHI,[1] MD, Akira YAMADA,[2] MD, Shuuichi OKAMATSU,[2] MD, *and* Kenji SUNAGAWA,[1] MD

SUMMARY

The no-reflow phenomenon during percutaneous coronary intervention (PCI) for acute myocardial infarction (AMI) causes impaired myocardial reperfusion. The aim of the present study was to evaluate the impact of thrombectomy on the prevention for no-reflow phenomenon and for LV remodeling. We performed a retrospective study comparing 116 patients treated for AMI with conventional angioplasty and 89 patients treated for AMI with the combination of angioplasty and thrombectomy. We performed manual aspirating thrombectomy using Thrombuster II. Baseline clinical and lesion characteristics were similar in the 2 groups. No-reflow phenomenon was significantly reduced in the thrombectomy group compared to the controls (8% versus 18%, $P < 0.05$). Maximum group mean CK was not significantly different between the two groups. During 6 months of follow-up, the mean LV ejection fractions of the 2 groups were not significantly different. However, in the cases involving the proximal left anterior descending (LAD) and right coronary arteries, changes in LV end-diastolic volume index (LVEDVI), LV end-systolic volume index, maximum CK and the incidence of LV remodeling, defined as an increase in LVEDVI of > 20%, were significantly lower in the thrombectomy group than in the control group. Multiple logistic regression analysis indicated that thrombectomy with Thrombuster II significantly reduced the no-reflow phenomenon and LV remodeling. These results suggest that adjunctive pretreatment with a manual aspirating thrombectomy by Thrombuster II reduces the no-reflow phenomenon, and in cases involving the LAD and right coronary arteries, protects against LV remodeling in AMI. (Int Heart J 2007; 48: 287-302)

Key words: Acute myocardial infarction, Thrombectomy, Thrombus

PREVIOUS studies have shown that direct coronary angioplasty to improve

From the [1] Department of Cardiovascular Medicine, Kyushu University Graduate School of Medical Sciences, [2] Division of Cardiovascular Medicine, Aso-Iizuka Hospital, Fukuoka, Japan.

Address for correspondence: Takuya Kishi, MD, Department of Cardiovascular Medicine, Kyushu University Graduate School of Medical Sciences, 3-1-1 Maidashi, Higashi-ku, Fukuoka 812-8582, Japan.

Received for publication December 18, 2006.

Revised and accepted March 8, 2007.

blood flow in infarction-related coronary artery reduces the mortality and morbidity of acute myocardial infarction (AMI),[1-6] however, this strategy has its limitations, namely, no-reflow phenomenon including slow flow, no flow, and distal embolism.[7,8] The no-reflow phenomenon was reported to be a predictive factor for poor prognosis in AMI[9-11] and is defined as a reduction of coronary flow due to the embolism of thrombus and plaque without mechanical obstruction.[7,8,10,12-14] No-reflow causes progressive left ventricular (LV) dysfunction and remodeling,[10,11] resulting in a significantly worse prognosis and quality of life after AMI.[4,9-11,15]

Recent advances in percutaneous techniques and devices have improved the acute outcome of percutaneous coronary intervention (PCI). One such device is a thrombectomy system for thrombus in a coronary artery. A previous study demonstrated that primary angioplasty with adjunctive percutaneous thrombectomy therapy using the Rescue catheter (Boston Scientific Scimed Inc., Minneapolis, USA), which is widely used as a thrombectomy catheter, is safe and achieves prompt flow restoration and suppresses LV remodeling through reduction of the no-reflow phenomenon.[16] It was also reported that thrombectomy using a TVAC system (NIPRO, Tokyo) is feasible, safe, and may have the potential to enhance ST segment resolution in patients with anterior AMI.[17] Moreover, primary implantation of a stent with distal protection using a PercuSurge GuardWire (Medtronic, Santa Rosa, CA, USA) can restore epicardial coronary flow and myocardial perfusion and also preserve LV function in AMI.[18,19] Since April 2003, we have been using Thrombuster II as a catheter for percutaneous thrombectomy therapy (KANEKA Medix Corporation, Osaka, Japan) in our hospital. This system is widely used for thrombectomy therapy because it is simple and easy to use for manual aspiration of thrombus in the coronary artery without the use of mechanical devices. However, the effect of this device on the prevention of the no-reflow phenomenon in the acute phase and LV remodeling in the follow-up phase has not been evaluated. Moreover, the effects of thrombectomy on the no-reflow phenomenon and LV remodeling and the differences between different coronary arteries have not been evaluated.

The aim of this study was to determine the effects of percutaneous thrombectomy therapy using a manual aspirating thrombectomy system (Thrombuster II) on the no-reflow phenomenon in the acute phase and for LV remodeling, major adverse cardiac events (MACE), and the incidence of heart failure in the follow-up phase, and to determine whether the effects were different between the proximal left anterior descending (LAD), distal LAD, left circumflex (LCX), proximal right coronary artery (RCA), and distal RCA.

METHODS

Thrombectomy catheter system: Thrombuster II is a short-monorail catheter with a lumen for aspiration. It is available in 2 sizes compatible with 6Fr and 7Fr guiding catheters. The distal end of the aspiration catheter is cut diagonally to facilitate aspiration. At the proximal end, continuous negative pressure is applied by a syringe, which is fixed at a negative pressure position. The aspirated thrombus is collected into the syringe. In our hospital, we have used 6Fr Thrombuster II.

Patient population: The patient population was a nonrandomized retrospective cohort comprising consecutive patients presenting to the Aso-Iizuka Hospital for AMI. The enrollment criteria included 1) patients aged 18 years of age or older with AMI presentation more than 30 minutes but less than 6 hours after symptom onset, 2) 2 mm or more ST-segment elevation in 2 or more contiguous leads or with presumably new left bundle-branch block, and 3) LV asynergy detected by echocardiogram. Patients whose baseline angiography demonstrated Thrombolysis In Myocardial Infarction (TIMI) grades 0 to 2 were included. A patient was considered to have thrombus if TIMI thrombus grades 2 to 5 were present.[20] Patients with cardiogenic shock and left main coronary artery disease were excluded. Between January 2004 and June 2005, 158 patients met the above criteria, and 123 patients underwent thrombectomy using Thrombuster II. The remaining 35 patients were excluded due to small caliber, tortuous culprit vessels, failure to wire-cross, or failure to aspirate a visible thrombus. After wire-cross, in all the cases in which the TIMI thrombus grade was 0 or 1, visible thrombi were not aspirated. Among the 123 treated patients, 89 were followed for 6 months after PCI and follow-up coronary angiography was performed at 6 months after PCI even if they did not have any symptoms. These 89 patients were defined as the thrombectomy group. Between January 2002 and June 2003, we did not perform thrombectomy prior to the coronary angioplasty because the equipment used for thrombectomy was not available at our hospital. In this period, 165 patients met the above criteria, and of these the 139 patients who underwent traditional coronary angioplasty were considered the control group. The remaining 26 patients were excluded due to small caliber, tortuous culprit vessels, failure to wire-cross, and TIMI thrombus grade 0 or 1. Among the 139 treated patients, 116 were followed for 6 months after PCI and follow-up coronary angiography was performed at 6 months after PCI even if they did not have any symptoms. These 116 patients were defined as the control group.

Coronary angioplasty and interventions: Coronary angiography and left ventric-

ulography were performed using standard techniques after oral administration of 200 mg of aspirin and intravenous administration of 3,000 U of heparin. All of the patients in this study were treated with nicorandil. To facilitate angioplasty, additional heparin (7,000 U) was administered and a 6Fr or 7Fr guiding catheter was inserted. A standard 0.014-inch guidewire was used to cross the lesion. A Thrombuster II catheter was advanced over the wire to the distal vessel and slowly withdrawn under negative suction, and then the clot was aspirated into the guiding catheter. This process was repeated several times. After thrombectomy therapy, the lesion was dilated with a balloon and/or stent. The aspirated thrombi were fixed in formalin buffer solution and pathology samples were prepared. These materials were stained with hematoxylin and eosin. Each sample was observed under a light microscope, and the platelet, erythrocyte, and atherosclerosis components were evaluated. A platelet-rich thrombus was defined as that in which the platelet component was at least twice that of the erythrocyte component, an erythrocyte-rich thrombus was defined as that in which the erythrocyte component was at lease twice that of the platelet component, and all others were defined as a mixed thrombus.[21] A thrombus size under 4 mm was defined as small, and a thrombus size equal to or greater than 4 mm was defined as large.[21] Among the 205 patients, 187 patients received ticlopidine (200 mg/day) and aspirin (100-200 mg/day) for 3 months after the procedure. The remaining 18 patients showed adverse reactions to ticlopidine, and all of them were switched from ticlopidine to cilostazol (200 mg/day). Clinical events were monitored throughout the hospitalization period and patients were followed-up for 6 months after discharge. Coronary angiography was performed if a patient had chest symptoms. Six months after the PCI, we performed follow-up coronary angiography and left ventriculography in patients without symptoms, whenever possible. In our hospital, we attempt to perform follow-up coronary angiography and left ventriculography 6 months following PCI. Heart failure was diagnosed according to the Framingham criteria.[22] The diagnosis of heart failure according to the criteria required that two major or one major and two minor criteria be present concurrently. Minor criteria were acceptable only if they could not be attributed to another medical condition. Major criteria were paroxysmal nocturnal dyspnea, neck vein distention, rales, radiographic cardiomegaly, acute pulmonary edema, S3 gallop, increased central venous pressure > 16 cm H_2O, circulation time > 25 seconds, hepatojugular reflux, pulmonary edema, visceral congestion, or cardiomegaly at autopsy, and weight loss > 4.5 kg in 5 days in response to treatment for heart failure. Minor criteria were bilateral ankle edema, nocturnal cough, dyspnea on ordinary exertion, hepatomegaly, pleural effusion, decrease in vital capacity by one-third from the maximal value recorded, and tachycardia (rate > 120 beats/min).[22]

Quantitative analysis: Blood flow in the infarct-related artery was evaluated pre- and postoperatively by TIMI grade in the coronary angiography. Patients were diagnosed as having angiographic no-reflow phenomenon if they showed an incomplete flow restoration (TIMI grade 0 to 1) after intervention. Distal embolism was diagnosed as a transient or sustained cut-off of a small branch after intervention. Side branch loss was diagnosed as the manifestation of embolism in a side branch after intervention. The proximal LAD was defined as the vessel between the LCX take off and the first major septal or diagonal branch. Proximal RCA was defined as the vessel before the first major right ventricular branch. The LV end-diastolic volume index (LVEDVI), end-systolic volume index (LVESVI), and left ventricular ejection fraction (LVEF) were obtained from LV ventriculography using the area-length method after angiography and PCI. LV remodeling was defined as a greater than 20% increase in the LVEDVI in the follow-up phase, as described in a previous study.[16] Coronary angiography and left ventriculography results were interpreted by at least 3 independent cardiovascular specialists.

Table I. Patient Characteristics

	Thrombectomy (n = 89)	Controls (n = 116)	P
Age (years)	66 ± 11	64 ± 7	NS
Male/female	66/23	84/32	NS
Diabetes mellitus	24 (27%)	36 (31%)	NS
Systemic hypertension	62 (70%)	72 (62%)	NS
Hyperlipidemia	47 (53%)	56 (48%)	NS
Current smoking	51 (57%)	55 (47%)	NS
Symptom onset to balloon time (hours)	6.9 ± 4.4	6.7 ± 5.3	NS
Infarct-related coronary artery			
Proximal/Distal LAD	23 (26%)/20 (22%)	29 (25%)/24 (21%)	NS/NS
Proximal/Distal RCA	21 (24%)/11 (12%)	26 (22%)/15 (13%)	NS/NS
LCX	14 (16%)	22 (19%)	NS
Initial TIMI grade 0	61 (68%)	109 (71%)	NS
Killip class > I	13 (15%)	19 (14%)	NS
Forrester subset I/II	56 (63%)/25 (28%)	71 (61%)/37 (32%)	NS/NS
III/IV	5 (6%)/3 (3%)	5 (4%)/3 (3%)	NS/NS
Use of IABP	5 (6%)	8 (7%)	NS
Discharge medications			
ACE-I or ARB	84 (94%)	111 (96%)	NS
Beta-blocker	74 (83%)	94 (81%)	NS

Continuous data presented as the mean ± SD and are compared using the Wilcoxon rank sum test; categorical data are presented as frequency values and are compared using the Fisher exact test. LAD indicates left anterior descending coronary artery; RCA, right coronary artery; LCX, left circumflex coronary artery; TIMI, thrombolysis in myocardial infarction; IABP, intra-arterial balloon pumping; ACE-I, angiotensin converting enzyme inhibitor; and ARB, angiotensin II receptor blocker.